COMPUTER SCIENCE PUBLICATION

VISUALIZATION OF ERRORS ON FORM-FACTOR COMPUTATION

K.W. Wong and W.W. Tsang

Technical Report TR-93-02

February 1993

DEPARTMENT OF COMPUTER SCIENCE
FACULTY OF ENGINEERING
UNIVERSITY OF HONG KONG
POKFULAM ROAD
HONG KONG

Visualization of Errors on Form-Factor Computation

K.W.Wong and W.W.Tsang
Department of Computer Science
The University of Hong Kong
Hong Kong
(email: kwwong@csd.hku.hk , tsang@csd.hku.hk)

ABSTRACT

This paper compares the form-factors obtained using the hemi-cube and the ray tracing methods with the exact values computed according to the analytical formula. The experiments are conducted for both non-blocking and partial blocking cases. The errors obtained are then displayed using volume rendering techniques. These pictures give strong clues to the magnitude and the sources of the errors. We found that the errors of the hemi-cube method depend on the the aspect ratio of the source patch, the normalized distance between the source and a receiving patch, and the degree of partial blocking. Aliasing effect is observed in the pictures obtained using the ray tracing method. The seriousness depends on the number and the distribution of the sample disks. Moreover, the approximated formula of the ray tracing method may introduce as much as 15% of relative errors. Guidelines for reducing errors in using the two methods are suggested.

Key Words: radiosity, form-factor, hemicube, ray tracing.

1. Introduction

Nowadays most computer graphics workstations support illumination calculations. The intensities are usually computed based on simple lighting models, including ambient light, diffuse reflection and specular reflection. However, most of these calculations have limitations. Firstly, they only provide point light sources and parallel light sources. Light sources with area are not supported. Secondly, there is an underlying assumption that every light source is visible to all surfaces in the environment. Thus, no shadow is generated. Thirdly, the interactions of light between diffuse surfaces are barely considered using a global ambient term which produces a less realistic picture.

In order to generate more realistic images, the physical behavior of visible light must be modeled in a more detailed way. Goral et al.[6] and Nishita and Nakamae [8] proposed a rendering method called *radiosity*. This method accurately takes into account of the interactions of light between diffuse surfaces and generates very realistic images for in-door scenes of soft lighting. All the three limitations mentioned in last paragraph are overcome.

A key step in the radiosity method is to calculate a matrix of values, called *form-factors*. The form-factor between two patches i and j, denoted as F_{i-j}, is defined as the fraction of energy leaving patch i that arrives at patch j. The complexity of the radiosity method is dominated by the form-factor calculation. However, as we will see in Section 2, the form-factor formula involves a double integral and thus is difficult to be computed in a straightforward way. Many methods have been suggested for estimating form-factors efficiently. The first one is the *hemi-cube* method [3]. It assumes that light is emitted from a very small area at the center of the source patch. The visibility is determined using the depth-buffer technique and the value of a form-factor is obtained by numerically sampling. The second one is the ray tracing method [13]. It approximates the radiosity of an area light source with many small circular disks. The visibility is determined by casting rays from the centers of disks to the vertices of a receiving patch. The third method is obtained from the analytical formula of form-factors. When there is no obstacle between a source patch and a destination patch, the form-factor formula can be simplified into a form which is easily computed [1]. This approach can be extended to handle cases with obstacles when efficiency is not a concern.

The quality of the image generated using the radiosity method depends on the accuracy of form-factors calculated. The violations of the underlying assumptions in various methods induce errors in the form-factors computed. The objective of our study is to visualize the magnitude and orientation of these errors and identify their sources. We hope to generalize guidelines for avoiding large errors in applying these methods.

Apart from the estimation of form-factors, many works have been done on improving the radiosity method. Cohen et al.[5] have developed a progressive refinement algorithm which avoids the calculation of the entire form-factor matrix. The algorithm proceeds in iterations. In each round, a bright patch whose light energy has not yet been taken into account is chosen to *shoot* its light out. The form-factors from this patch to all the others are calculated and the intensities of the patches are recorded. Instead of computing and storing n^2 form-factors, this method only requires to keep track of n form-factors in each iteration. Furthermore, it converges very fast

to the accurate solution, and image can be displayed before an accurate solution is found. They have also proposed a *substructuring* technique and an adaptively subdividing scheme [4] for dividing a patch into appropriate size automatically, when large gradient of radiosity is found over a patch. Their method improved the quality of a picture without increased the size of the form-factor matrix. Many researchers have studied how to illuminate a scene with both diffuse and specular reflection [7,9,10,12,14]. These works make the radiosity method become an essential part in scene illumination.

Section 2 reviews the formulation of the form-factor in the radiosity method. Three methods for computing form-factors are described in Section 3. The underlying assumptions of these methods are also included. In Section 4, we highlight the errors induced by the hemi-cube method and the ray tracing method by displaying the iso-energy surfaces of several light emitting patches in a convex environment, i.e., an environment without blocking. A study of the effect of obstacle in the estimations is conducted in Section 5. Lastly, we give our conclusions in Section 6.

2. Formulation of Form-Factors

Radiosity is defined as the amount of energy leaving a surface per unit time per unit area. It is the sum of the rate at which the surface emits energy and the rate it reflects the energy received from the environment. Assume that each patch in the environment is an ideal diffuse surface. For surface i, its radiosity can be expressed as in [6]:

$$B_i = E_i + \rho_i \sum_j B_j F_{j\text{-}i} \frac{A_j}{A_i}$$

where

B_i = radiosity of patch i (W/m^2)
E_i = emittance of patch i (W/m^2)
A_i = area of patch i (m^2)
ρ_i = reflectivity of patch i
$F_{j\text{-}i}$ = the fraction of energy leaving patch j that arrives at patch i

The interaction of light among all the n patches in the environment can then be expressed as a set of linear equations:

$$\begin{pmatrix} 1-\rho_1 F_{1\text{-}1} & -\rho_1 F_{1\text{-}2} & \cdots & -\rho_1 F_{1\text{-}n} \\ -\rho_2 F_{2\text{-}1} & 1-\rho_2 F_{2\text{-}2} & \cdots & -\rho_2 F_{2\text{-}n} \\ \cdot & \cdot & & \cdot \\ \cdot & \cdot & \cdots & \cdot \\ \cdot & \cdot & & \cdot \\ -\rho_n F_{n\text{-}1} & -\rho_n F_{n\text{-}2} & \cdots & 1-\rho_n F_{n\text{-}n} \end{pmatrix} \begin{pmatrix} B_1 \\ B_2 \\ \cdot \\ \cdot \\ \cdot \\ B_n \end{pmatrix} = \begin{pmatrix} E_1 \\ E_2 \\ \cdot \\ \cdot \\ \cdot \\ E_n \end{pmatrix}$$

An approximation of the root of the equations can be obtained using Gauss-Seidel iteration.

According to the assumption that all patches are ideal diffuse (Lambertian) surfaces, the form-factor between two differential areas dA_i and dA_j (Figure 2.1) is found to be:

$$F_{dA_i\text{-}dA_j} = \delta_{ij} \frac{\cos\theta_i \cos\theta_j dA_j}{\pi r_{ij}^2} \tag{1}$$

where

$\delta_{ij} = 1$ if dA_j is visible by dA_i, 0 otherwise.

A detailed derivation of Equation 1 can be found in [6].

The form-factor between two finite areas A_i and A_j can then be obtained by applying double integration over $F_{dA_i\text{-}dA_j}$.

$$F_{Ai\text{-}Aj} = F_{i\text{-}j} = \frac{1}{A_i} \int_{A_i} \int_{A_j} \delta_{ij} \frac{\cos\theta_i \cos\theta_j dA_j dA_i}{\pi r_{ij}^2}$$

3. Three Methods for Calculating Form-Factors

3.1. The hemi-cube method (HC)

The hemi-cube method is proposed by Cohen et al.[3]. The key assumption of the method is that if two patches are far away from each other, all the energy emitted from the source can be thought as emitting from the center of the source. The form-factor between two patches can then be approximated by the form-factor between a

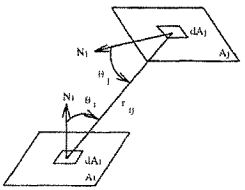

Figure 2.1. Geometry for From-Factor Derivation

differential area at the center of the source and the destination. Moreover, the visibility between the source and a patch is determined by the visibility between the source center and the patch. Based on this assumption, the form-factor between two patches is:

$$F_{A_i\text{-}A_j} \approx F_{dA_i\text{-}A_j} = \int_{A_j} \delta_{ij} \frac{\cos\theta_i \cos\theta_j dA_j}{\pi r_{ij}^2} \tag{2}$$

A numerical method is suggested for the evaluation of the integration in Equation 2. It is observed that when patches are projected onto a surrounding surface of a source, if their projections occupy the same area and location, the form-factors between the source and the patches will be equal. Therefore, patches are projected onto a hemi-cube placed above the center of the source. The cube is discretized into small elements called pixels. The form factor between the source center and a pixel, denoted *dF*, is called *delta form-factors*. The delta form-factors are pre-computed. The form-factor from source patch *i* to destination patch *j* is then equal to the sum of *dF* associated with the pixels covered by the projected image of patch *j*. Visibility of patches are determined using the depth-buffer technique for hidden surface removal. As the projections and the depth-buffer algorithm are supported by most graphics hardware, the hemi-cube method runs efficiently in graphics machines. This approach really makes the radiosity method practical in complex environment.

A disadvantage of the hemi-cube method is that the basic assumption, i.e., the source and destination is far away from each other, does not always hold. When the source and destination are too close, the form-factor computed is incorrect (Figure 3.1

and Figure 3.2). The normalized distance in figure 3.2 is the distance between the source and the destination, divided by the area of the source. A more detailed discussion on the accuracy of the hemi-cube method can be found in [1].

The resolution of the hemi-cube also affects the accuracy of the form-factors calculated. When the resolution is low, artifact caused by the aliasing effect is found in

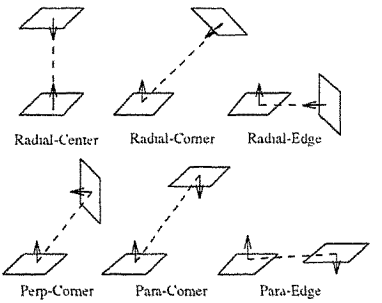

Figure 3.1. Geometric orientations used to generate Figure 3.2 and Figure 3.3.

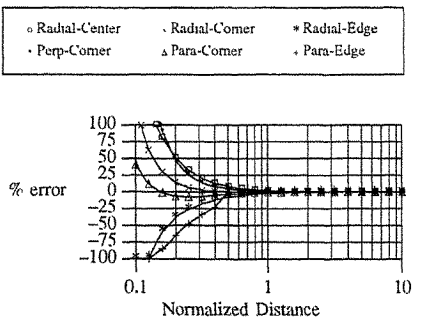

Figure 3.2. Relative errors in the form-factors computed by using Equation 2 (both the source and the receiving patch are of aspect ratio 1:1).

the image generated. Figure 3.3 shows the relative errors of form-factors due to the aliasing effect. The source has the same aspect ratio and size as the one in Figure 3.1. The only different is that Figure 3.2 is obtained by using Equation 2 directly, whereas Figure 3.3 is obtained by placing a hemi-cube over the source. The resolution of the top plane of the hemi-cube is 500×500. Note that when the destination patch is far away from the source, its projection may only partially overlap with one or few pixels. Thus, the relative errors caused by low resolution are indeed magnified when the patches are far from each other. Fortunately, when a patch is far away from a source, its form-factor is small and a large relative error will not seriously affect the quality of the image.

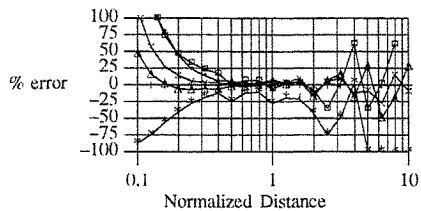

Figure 3.3. Relative errors in the true form-factor values computed by the HC method.

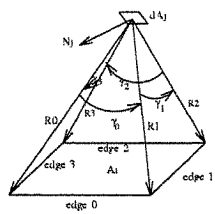

Figure 3.4. Geometry for evaluating analytical form-factor

3.2. The analytical method (ANA)

When two patches are close to each other, the errors in the form-factors computed using the hemi-cube method can be very large. Baum et al.[1] has proposed to use an analytical method for the evaluation of delta form-factors when two patches are closer than a threshold value. The formula of form-factor between differential area dA_j and patch i as shown in Figure 3.4 is:

$$F_{dA_j\text{-}A_i} = \frac{1}{2\pi} \sum_{g \in G_i} N_j \cdot \Gamma_g \tag{3}$$

where

G_i is the set of edges in patch i;
N_j is the surface normal for differential surface dA_j;
Γ_g is a vector with magnitude equal to the angle γ (in radians) and direction equal to the cross product of the vectors R_g and R_{g+1} as shown in Figure 3.4.

A detailed derivation of Equation 3 can be found in [11].

This formula assumes that there is no blocking between the source and the differential area. Otherwise, the source patch is subdivided until all the subpatches are either completely visible or invisible from dA_j. The form-factor $F_{dA_j\text{-}A_i}$ is then equal to the sum of the form-factors from dA_j to all visible subpatches. In practice, when the size of a subpatch is smaller than a threshold value, we assume that it is either fully visible or invisible from the dA_j.

3.3. The ray-tracing method (RT)

Wallace et al.[13] has suggested a different method for computing form-factors. Light emitted or reflected by a source patch is assumed to be emitting from several circular disks which are evenly distributed on the patch. The visibility of a differential area and a disk is determined by casting a ray from the center of the disk to the area. The form-factor of the receiving patch is computed by considering all the light received from the visible disks.

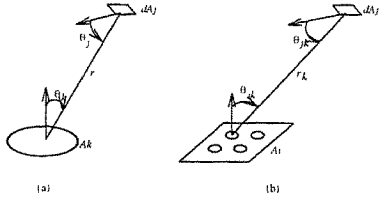

Figure 3.5. a) Geometry for form-factor between an arbitrarily oriented disk and differential area.

b) Geometry for form-factor between a source patch (approximated by multiple disks) and a differential area.

The form-factor between circular disk k and differential area dA_j (Figure 3.5a) can be approximated as:

$$F_{A_k\text{-}dA_j} \simeq \frac{dA_j \cos\theta_j \cos\theta_k}{\pi r^2 + A_k} \tag{4}$$

The form-factor between source patch i and vertex j (Figure 3.5b) is:

$$F_{A_i\text{-}dA_j} = dA_j * \frac{1}{N} \sum_k \delta_k \frac{\cos\theta_{jk} \cos\theta_{ik}}{\pi r_k^2 + \frac{A_i}{N}} \tag{5}$$

where

N = number of sample point used on the source patch
δ_k = 1 if the ray can reach sample point k; 0 otherwise

Instead of computing the radiosities at the centers of patches and then obtaining the vertex intensities using interpolation [3], the radiosities at the vertices of patches are computed directly in this method. The intensities at the other positions of a patch are obtained later by making use of the interpolating facility provided by the graphics hardware.

4. Errors in Environment Without Blocking

For comparison purpose, we assume that there is a light-emitting patch i in the environment (Figure 4.1). Then we apply the various methods to calculate the energy received by a very small patch dA_j in the vicinity of patch i. The area of patch i is one unit and it emits one unit of energy per unit time (i.e., $B_iA_i = 1$). The area of patch dA_j is 0.0001 unit and it always points at the center of patch i. The formulas of the energy received by patch dA_j using the three different methods are given below. Note that in this particular case, the form factor is equal to the energy received and the analytical method gives the exact value.

(1) The Hemi-Cube method

energy received by j

$$B_iA_iF_{i\text{-}dA_j}$$

$$= \frac{\cos\theta_c \cos\theta_j dA_j}{\pi r_{cj}^2} \qquad \textit{by Eq. 2 and Eq. 1}$$

$$= \frac{\cos\theta_c dA_j}{\pi r_{cj}^2}$$

where c is the center of patch i.

(2) The Analytical formula

$$B_iA_iF_{i\text{-}dA_j}$$

$$= F_{i\text{-}dA_j}$$

$$= F_{dA_j\text{-}i} * \frac{dA_j}{A_i}$$

where $F_{dA_j\text{-}i}$ is given by Equation 3.

(3) The Ray Tracing method

$$B_i A_i F_{i\text{-}dA_j}$$

$$= dA_j * \frac{1}{N} \sum_{k=1}^{N} \frac{\cos\theta_{ik}\cos\theta_{jk}}{\pi r_{jk}^2 + \frac{A_i}{N}} \qquad \textit{by Eq. 5}$$

where N is the number of sample points. The distributions of 3 or 9 sample points on source patch of various aspect ratio are shown in Figure 4.2.

To visualize the errors, we drew the "isoenergy" surface around the source patch. In Figure 4.3, the locations where patch dA_j receives 0.8E-5 unit of energy was drew. The aspect ratio of the source patch is 1:1. The left one is the correct answer which was obtained using the ANA method. The right one was obtained using the HC method. As the size and shape of the two surfaces are similar, the errors induced by the HC method are negligible in this case.

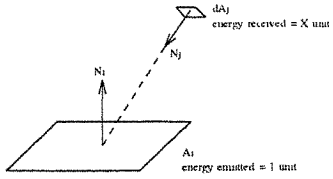

Figure 4.1. Energy received at a point over a light source.

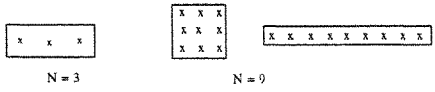

Figure 4.2. Distribution of sample points on source patches.

The drawings in Figure 4.4 were obtained in the same way except that the energy received was raised to 3.0E-5 unit. The isoenergy surfaces obtained are closer to the source patch. Note that the HC method overestimated the energy received right above the center of the source patch, and underestimated the energy received around the edges of the source patch. The is due to the assumption of the HC method that energy is emitted from the center of the source patch. In Figure 4.5, the isoenergy surfaces of the same energy level as Figure 4.3 were drew for a source patch of aspect ratio 1:3. As the HC method does not take into account of the shape of the source patch, there is no surprise that the errors increase when the aspect ratio of the source patch becomes larger.

In order to study how the errors induced by the HC method are affected by the distance, we computed the energy received by patch dA_j at different locations of a cross section of space right above the source patch. The magnitude of the energy was rendered using a color scale. The cross section above a source patch of aspect ratio 1:3 is shown in Figure 4.6. Again, the one on the left was obtained using the ANA method and the one on the right was obtained using the HC method. It is clear that the errors diminish when the distance becomes larger.

The cross sections were computed again using the RT method. The result is shown in Figure 4.7, with a source patch of aspect ratio 1:3. The left one was obtained using the ANA method and the right one was obtained using RT method with three sample points. The right one is quite similar to the correct one on the left hand side. However, aliasing is observed at the positions very close to the surface of the source patch. In Figure 4.8, we drew the cross sections for a source patch of aspect ratio 1:9. The top one was obtained using the ANA method; the pictures in the bottom row were obtained using the RT method with three and nine sample points. The result shown in the bottom left picture is not acceptable as too few sample points were used. Also, the alaising effect in these drawings is significant. Further study shows that the distribution of the sample points plays an important role in the magnitude of the alaising effect. As a gerenal guideline, the sample points should be evenly distributed and each represents the radiosity of a squarely region of the source patch. Moreover, we found that the RT formula (Equation 4) may underestimate the amount of light by as much as 15% at some positions close to the source patch. This explain why the bottom drawings are not as bright as the upper one, especially at the position near the surface of the source.

5. Errors in Environment With Blocking

In an environment with blocking, we have to perform visibility test before we apply the form-factor formulas described in last section. In the HC method, the entire patch i is assumed visible to dA_j if the center of dA_j can been seen from the center of A_i. In the RT method, a light-emitting disk is assumed entirely visible to dA_j if the center of dA_j can been seen from the center of the disk. In the ANA method, if patch i is not entirely visible from the center of dA_j, it is subdivided recursively until each component is either completely visible or invisible. The total energy received is then equal to the sum of the energy received from the visible components.

In Figure 5.1, we show four drawings which display the energy received by dA_j at locations of a cross section of space above patch i. The size of patch i is 1×1 unit area. An obstacle patch of size 0.5×0.5 unit area is placed at 0.25 unit length above the centre of patch i.

The upper left drawing was obtained using the ANA method which gave the correct amount of energy received by dA_j. Note that only a small area right behind the obstacle is completely dark and the amount of energy change continuously. The upper right was obtained using the HC method. As light is assumed to be emitting from the center, a very large shadow area behind the obstacle is completely dark. Comparing with the upper left, it is obvious that the HC method underestimated the amount of energy in the shadow area. On the other hand, the method overestimated the value in the vicinity of the shadow which is marginally visible from the center of the patch. These errors are caused by the fact that the method fails to take into account of partial blocking in the formulation.

The lower left drawing in Figure 5.1 was obtained using the RT method with nine sample disks. Note that each disk induces sharp shadow as in the case of the HC method because the entire disk is either *seen* or *unseen* from a location. Discrete change of intensity is observed at the intersections of the shadow boundaries. Nonetheless, this drawing is closer to the correct one than the drawing obtained using the HC method.

It is interesting to find out why the RT method is more accurate than the HC method. Our study indicates that it is not due to the use of ray tracing technique for visibility test, nor the use of circular disks in radiosity calculation. The critical factor is that the RT method assumes that light is emitted from **nine** disks on the source instead of from the center of the source as assumed in the HC method. The lower

right drawing of Figure 5.1 was obtained using the HC method after cutting patch i into nine pieces. This drawing is as good as the one obtained using the RT method.

The drawings shown in Figure 5.2 were obtained in the same way as those in Figure 5.1 except that the obstacle was shifted to the right 0.25 unit length. These drawings confirm our findings in above discussions.

6. Conclusion

We have investigated the errors in the calculation of form-factors by the HC and RT methods in both convex and blocking environments. Attention were paid on three major factors: the normalized distance between the source and the destination, the aspect ratio of the source patch, and the aliasing effects.

The ANA method is used to obtain the exact values of form-factor in the comparison. The computation time is acceptable if there is no blocking between the source and destination. However, in an environment with blocking, the process of finding the visible portion of the source patches is time consuming. In a complex environment, this process is extremely slow even sophisticated data structures such as binary-space-partition trees are used. Thus, the ANA method is generally not practical.

Due to the assumption that light emits from the center of a source patch, the HC method gives accurate results only if the aspect ratio of the source patch is close to one, the normalized distance between the source patch and the receiving patch is large, and there is no partial blocking of the source patch. Moreover, the resolution of the hemi-cube has to be large enough. From our experience, the method gives acceptable results if the following conditions are satisfied: (i) the aspect ratio is between 1/2 and 2; (ii) the normalized distance is greater than 0.3; (iii) the amount of light energy emitted from any single patch is less than 5% of the total light energy emitted in the environment; (iv) the resolution of the hemi-cube surfaces is at least 500×500. A source patch shall be divided if any of the first three conditions is violated. A major advantage of the HC method is that it is by far faster than the other two methods as it can be implemented using the facility supported by graphics hardware.

The RT method generates more satisfactory results than the HC method mainly because it uses multiple circular disks to approximate a source patch. Another major

improvement is that the method computes the vertex radiosity instead of the patch radiosity. Such modification enables direct application of the intensity interpolation facility provided by graphics hardware. As ray tracing is a time consuming process, this method in general runs slower than the HC method. Moreover, aliasing is found in locations very close to a source patch. To obtain good results in applying this method, some guidelines similar to those given for the HC method should be followed. For example, each disk assoicates with a region close to a square; each disk emits no more than 5% of total light energy; the normalized distance between a disk and a vertex should be greater than 0.3.

Each of the three methods studied has its own advantages and shortcomings. We appreciate the framework of the RT method the most and will try to improve some of its steps with the better ideas adopted in other methods. In particular, use the depth-buffer technique to replace ray tracing for determining visibility. Moreover, an attempt will be made to eliminate the aliasing effect by using the analytical formula for computing the radiosity of the region associated with a sample disk. We are now in the progress of implementing these ideas and studying the performance of the resulting method.

REFERENCES

[1] Baum, Daniel R., Holly E. Rushmeier, James M. Winget, "Improving Radiosity Solutions Through the Use of Analytically Determined Form-Factors," *Computer Graphics (SIGGRAPH'89 Proceedings)*, Vol.23, No.3, July 1989, pp.325-334.

[2] Campbell, A.T. III, Donald S. Fussell, "Adaptive Mesh Generation for Global Diffuse Illumination," *Computer Graphics (SIGGRAPH'90 Proceedings)*, Vol.24, No.4, August 1990, pp.155-164.

[3] Cohen, Michael F., Donald P. Greenberg, "The Hemi-Cube: A Radiosity Solution for Complex Environments," *Computer Graphics (SIGGRAPH'85 Proceedings)*, Vol.19, No.3, July 1985, pp.31-40.

[4] Cohen, Michael F., Donald P. Greenberg, David S. Immel, Philip J. Brock, "An Efficient Radiosity Approach for Realistic Image Synthesis," *IEEE Computer Graphics and Applications*, Vol.6, No.2, March 1986, pp.26-35.

[5] Cohen, Michael F., Shenchang Eric Chen, John R. Wallace, Donald P. Greenberg, "A Progressive Refinement Approach to Fast Radiosity Image Generation," *Computer Graphics (SIGGRAPH'88 Proceedings)*, Vol.22, No.4, August 1988, pp.75-84.

[6] Goral, Cindy M., Kenneth E. Torrance, Donald P. Greenberg, Bennett Battaile, "Modeling the Interaction of Light Between Diffuse Surfaces," *Computer Graphics (SIGGRAPH'84 Proceedings)*, Vol.18, No.3, July 1984, pp.213-222.

[7] Immel, David S., Michael F. Cohen, Donald P. Greenberg, "A Radiosity Method for Non-Diffuse Environments," *Computer Graphics (SIGGRAPH'86 Proceedings)*, Vol.20, No.4, August 1986, pp.133-142.

[8] Nishita, Tomoyuki, Eihachiro Nakamae, "Continuous Tone Representation of Three-Dimensional Objects Taking Account of Shadows and Interreflection," *Computer Graphics (SIGGRAPH'85 Proceedings)*, Vol.19, No.3, July 1985, pp.23-30.

[9] Shao, M.Z., Q.S. Peng, Y.D. Liang, "A New Radiosity Approach by Procedural Refinements for Realistic Image Synthesis," *Computer Graphics (SIGGRAPH'88*

Proceedings), Vol.22, No.4, August 1988, pp.93-101.

[10] Shirley, Peter, "A Ray Tracing Method for Illumination Calculation in Diffuse-Specular Scenes," *Proceedings of Graphics Interface'90*, May 1990, pp.205-212.

[11] Siegel, Robert, John R. Howell, *Thermal Radiation Heat Transfer*, Hemisphere Publishing Corporation, New York, 1981.

[12] Sillion, Francois, C. Puech, "A General Two-Pass Method Integrating Specular and Diffuse Reflection," *Computer Graphics (SIGGRAPH'89 Proceedings)*, Vol.23, No.3, July 1989, pp.335-344.

[13] Wallace, John R., Kells A. Elmquist, Eric A. Haines, "A Ray Tracing Algorithm for Progressive Radiosity," *Computer Graphics (SIGGRAPH'89 Proceedings)*, Vol.23, No.3, July 1989, pp.315-324.

[14] Wallace, John R., Michael F. Cohen, Donald P. Greenberg, "A Two-Pass Solution to the Rendering Equation: A Synthesis of Ray Tracing and Radiosity Methods," *Computer Graphics (SIGGRAPH'87 Proceedings)*, Vol.21, No.4, July 1987, pp.311-320.

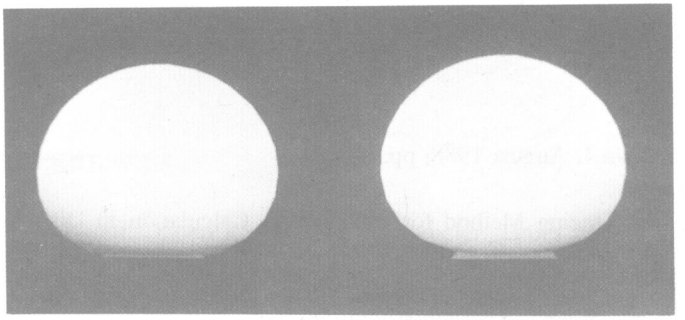

Figure 4.3

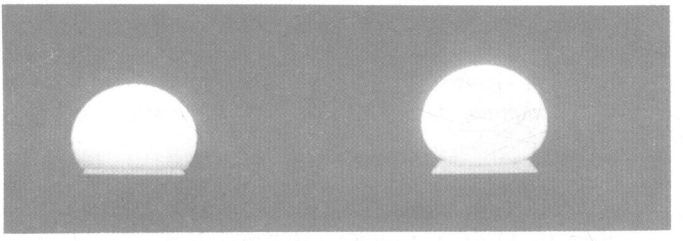

Figure 4.4

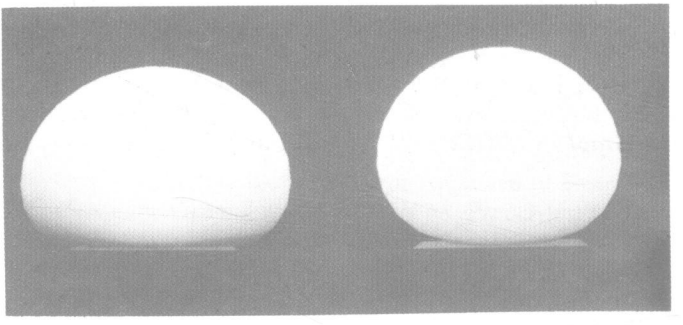

Figure 4.5

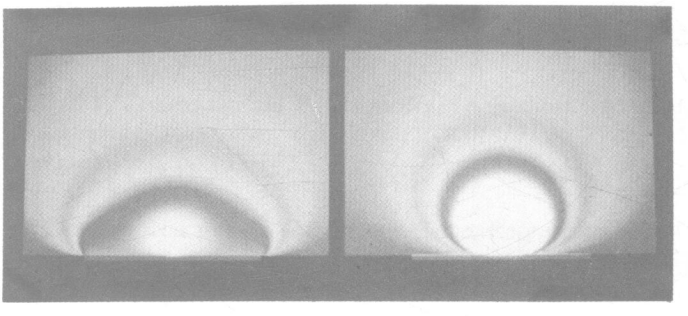

Figure 4.6

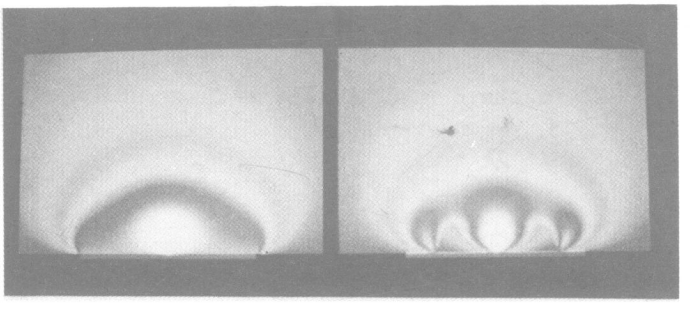

Figure 4.7

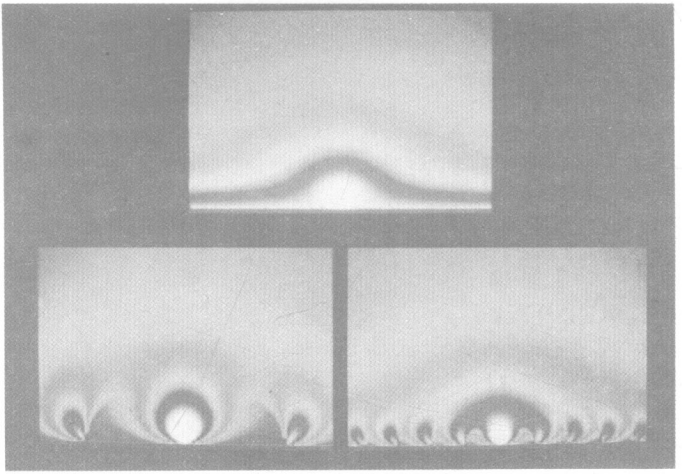

Figure 4.8

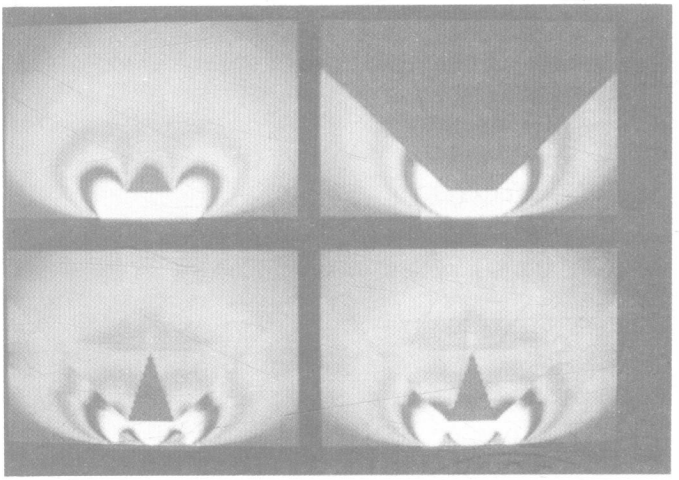

Figure 5.1

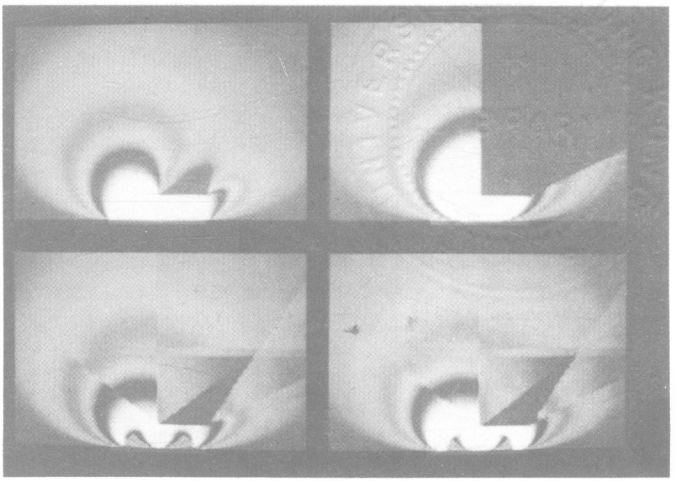

Figure 5.2